Report

2014 Annual WAMIT Consortium Meeting

October 1-2, 2014

Woods Hole, Massachusetts

Agenda for 2014 Annual WAMIT Meeting
Room 310, Marine Resource Center, Swope Center, Woods Hole, MA

October 1, 2014

9:00AM: Welcome

9:15AM: "Review of WAMIT Version V6.4S (released)"
C.-H. Lee, WAMIT Inc.

"Recent Progress for V7S"
X.M. Zhu, WAMIT Inc.

"WAMIT Interface Development"
K. Hendrickson, WAMIT Inc.

10:50 AM: Break

11:10 AM: "Plans for V7.1"
J.N. Newman, WAMIT Inc.

12:00PM: Lunch, Swope Center Dining Hall

1:30 PM "Pressure surface. A floating structure with
an air cushion & oscillating water columns."
C.-H. Lee, WAMIT Inc.

"Cloaking in the diffraction problem of water waves"
(Power Point Slides are not included in the report.)
J.N. Newman, WAMIT Inc.

"WAMIT applications at ConocoPhillips -
higher-order method & control surfaces"
(Power Point Slides are not included in the report.)
Scott Coblitz, ConocoPhillips Company

3:30 PM: Break

4:00 PM: "Technical discussion"

5:30PM: Mixer and Dinner, Swope Center Dining Hall

October 2, 2014

9:00AM: "What's New and What's Next in MultiSurf for WAMIT"
Robert Page, AeroHydro Inc.

10:30AM: Break

11:00AM: Business meeting

12:00PM: Lunch, Swope Center Dining Hall

Review

WAMIT V6.4S

(released)

1. Second-order analysis can be made for vessels with internal tanks with free surfaces.

- Full QTF with the effects of the internal tanks
- Second-order fluid pressure and wave elevation at the field points and on the tank walls
- Note: A Higher-order method is significantly more effective near tank resonance, as low order method is slowly convergence over significantly wide range of period near resonance.

Illustrative example - quadratic force on a vessel with 4 tanks (from previous results)

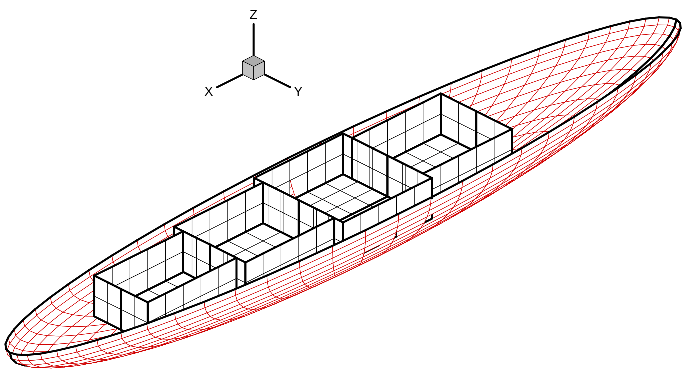

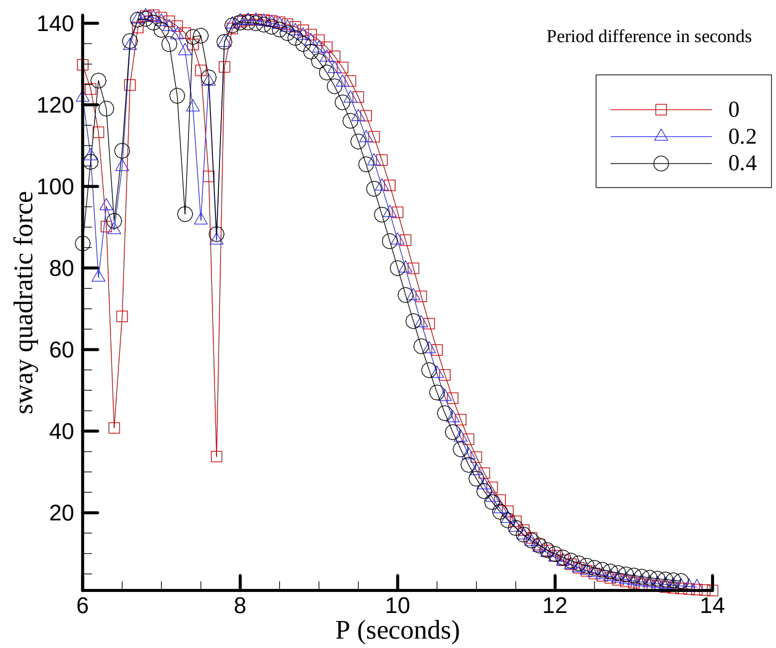

Sway force in beam sea

Sway force QTF matrix in a beam sea

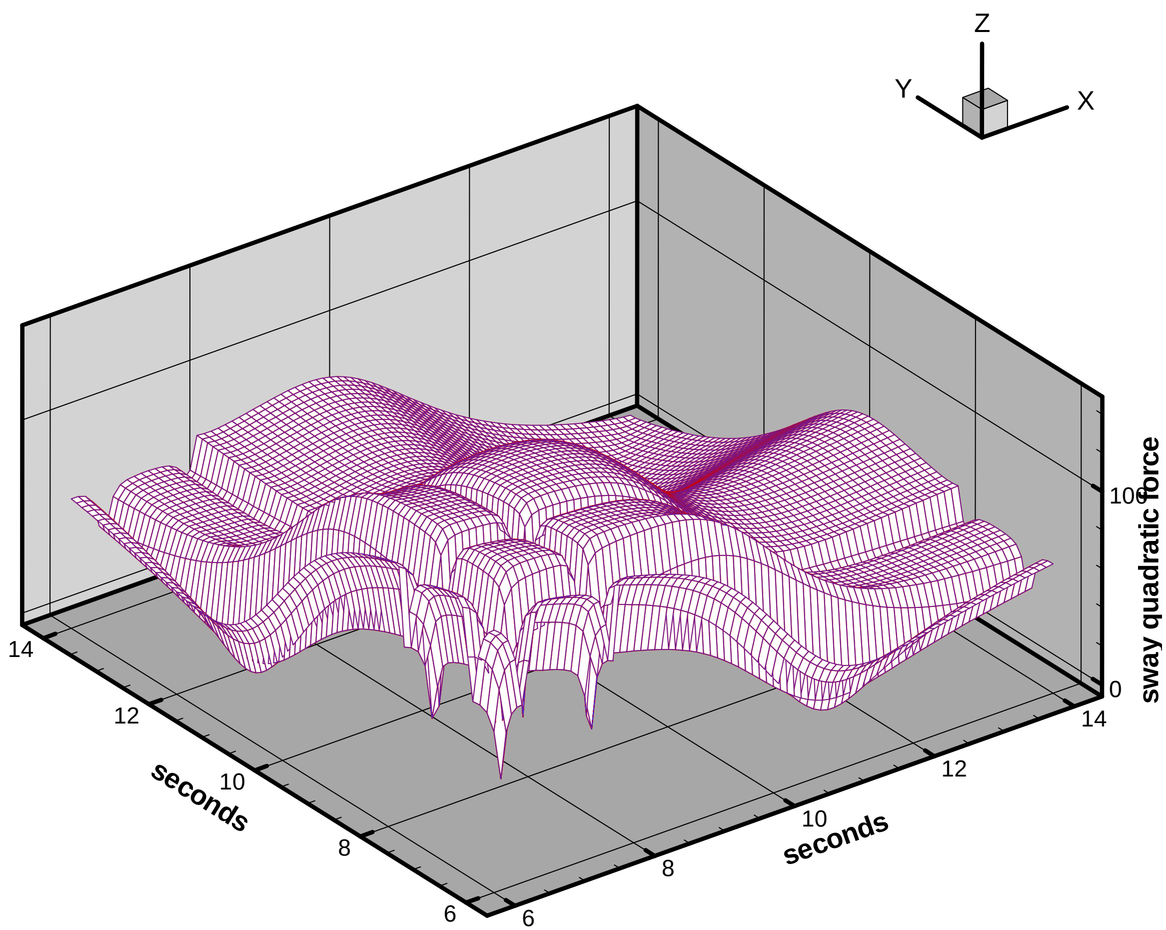

2. Control surfaces option for the evaluation of the quadratic forces.

- Evaluation of the pressure proportional to the product of two fluid velocity components is transferred to control surfaces. Accurate and efficient evaluation of the forces especially for bodies with corners.

- Unlike mean drift force, evaluation of the pressure proportional to fluid velocity remains on the body. This is term is small at difference frequency.

Truncated circular cylinder R=1, D=1 in bichromatic waves

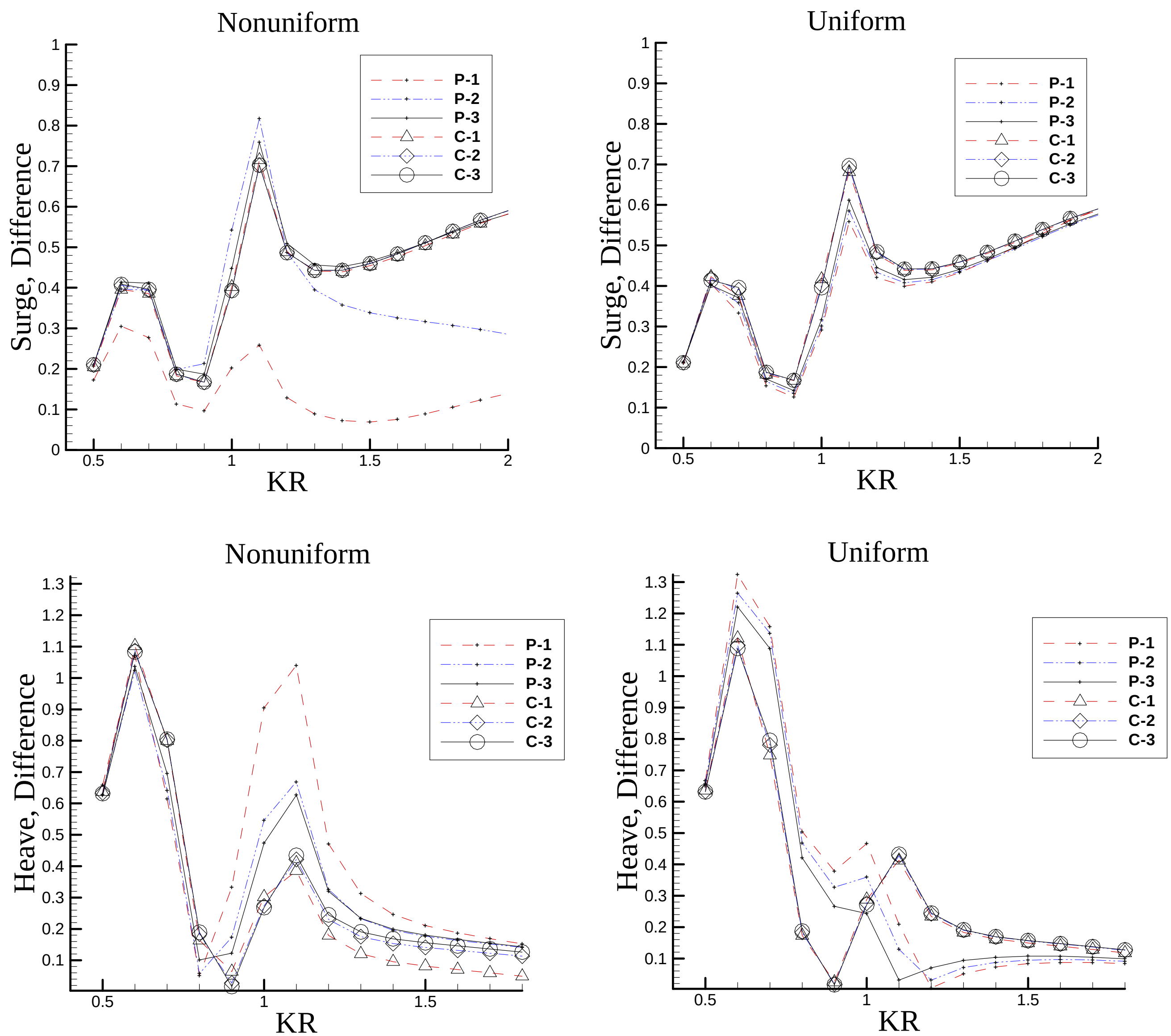

KR infinite depth wave number. ΔKR=0.4

Truncated circular cylinder R=1, D=1 in bichromatic waves

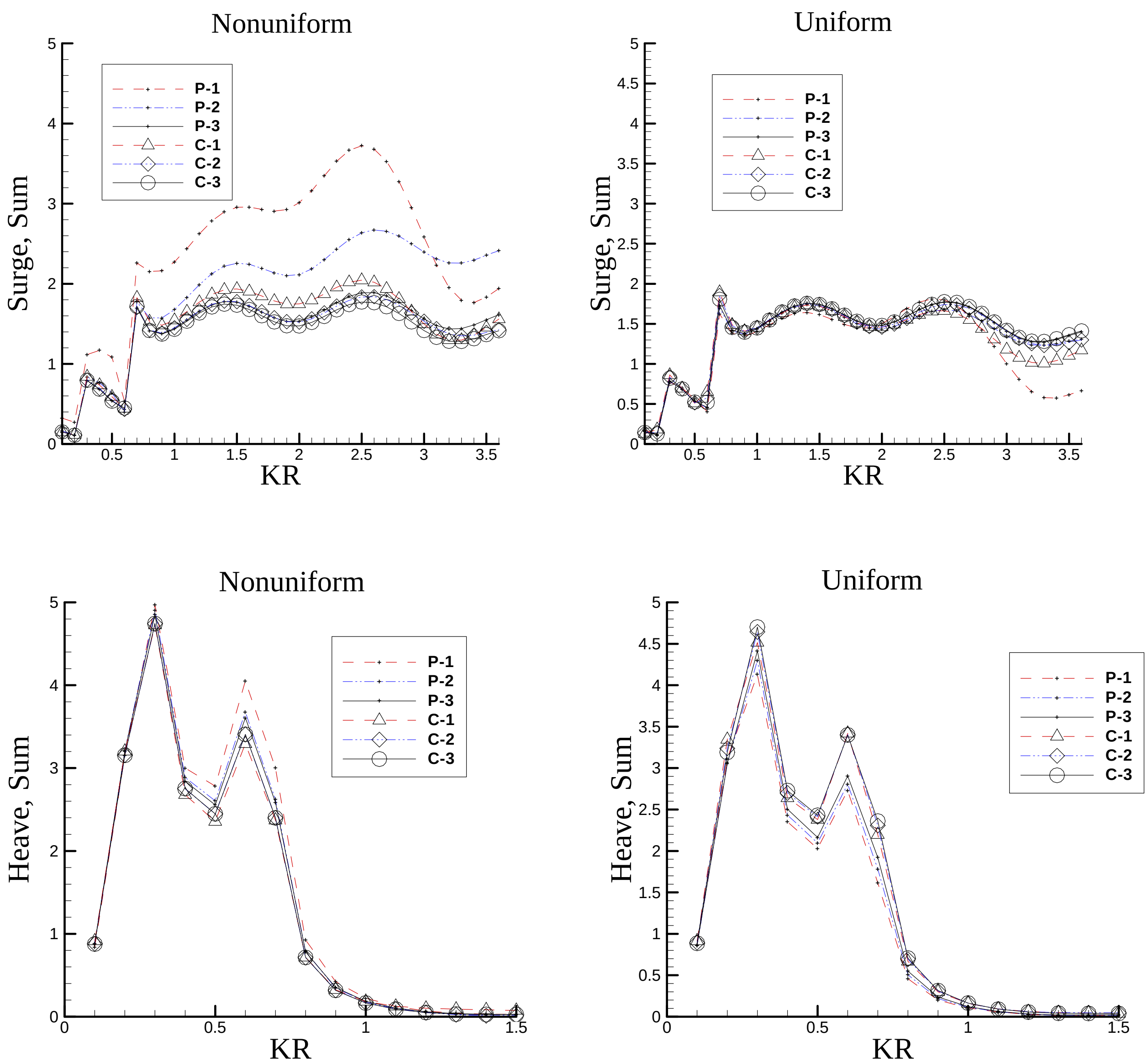

KR infinite depth wave number. ΔKR=0.4

3. Various geometry definitions for free surface geometry interior to a circle of radius RINNER and exterior to body (including tank free surface)

ILOWHI=0

1. Specify vertices of quarilateral panels in the FDF input file.

2. Automatic discretization in WAMIT

3. Specify the name of MS2 models In the FDF file. MulitSurf for WAMIT interface provides vertices of quadrilateral panels to WAMIT. (under development)

ILOWHI=1

1. Specify the surface in B-splines

2. Specify the geometry using a FORTRAN subroutine in FDEXACT.

3. Automatic description in WAMIT using ruled surfaces

4. Specify the name of MS2 models (under development))

4. In V6.1S, when ILOWHI=1, the second-order forcing terms are evaluated on the centroids of flat panels approximating the body and free surfaces.

In V6.4S, they are evaluated on the centroids of subdivided areas on the exact body and free surfaces without geometric approximation. (Convenient to compute the second-order wave elevation close to waterlines.)

Linear and Second-order Wave Elevation
Experiment & calculation by Kagemoto et al. (IWWWFB, 2013 & 2014)

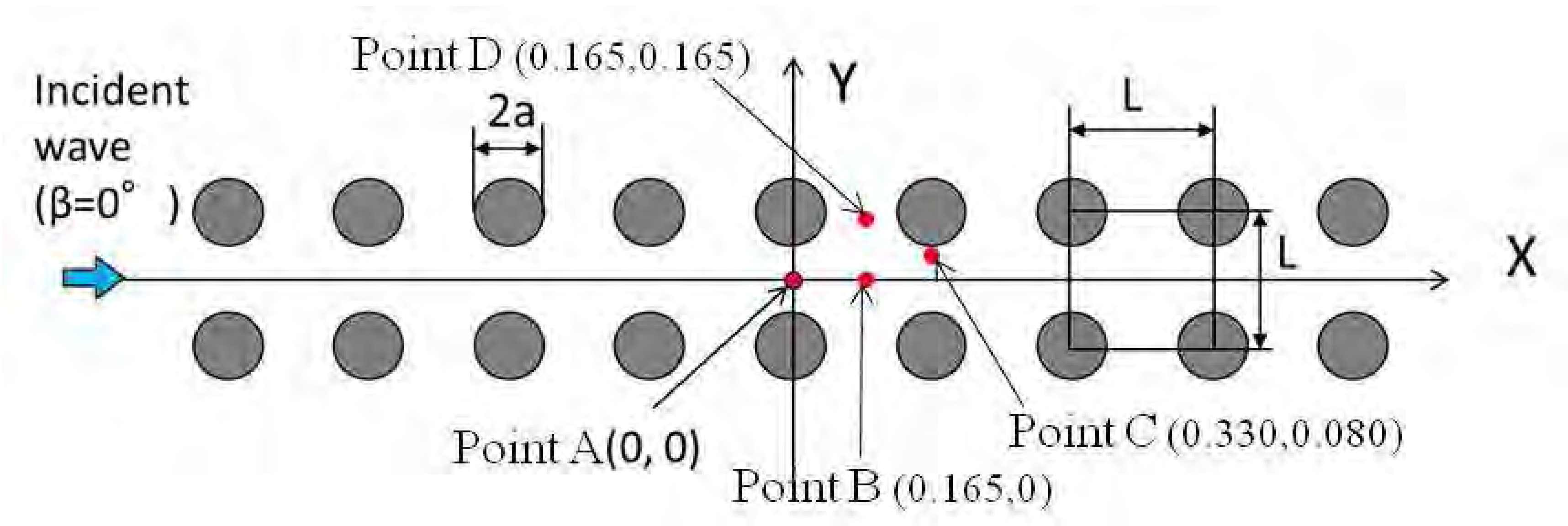

Wave Height=0.02 Point A
=0.01 Points B & C

Point A only Experiment & calculation by Kagemoto et al. (IWWWFB, 2013)

Near 0.73, 0.8 and 1.12 seconds are of interest

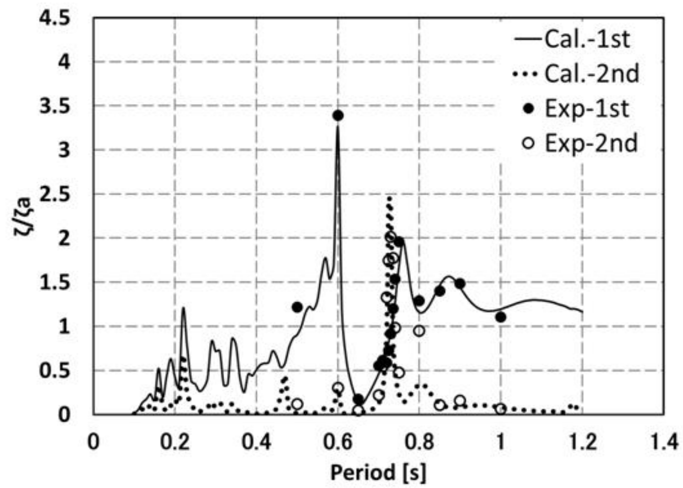

2 x 9 cylinders

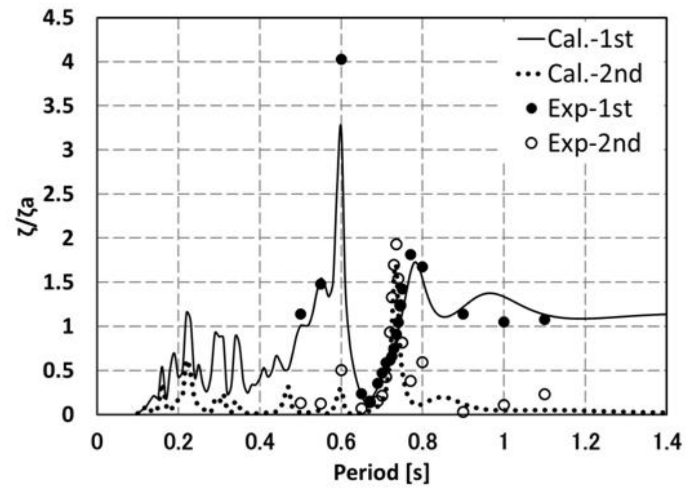

2 x 7 cylinders

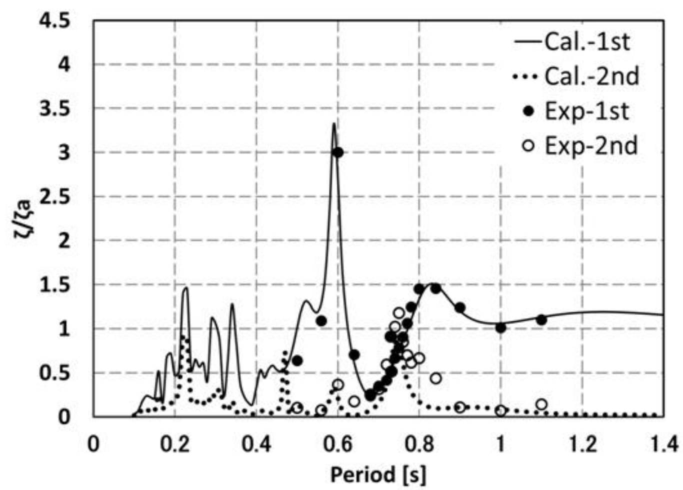

2 x 5 cylinders

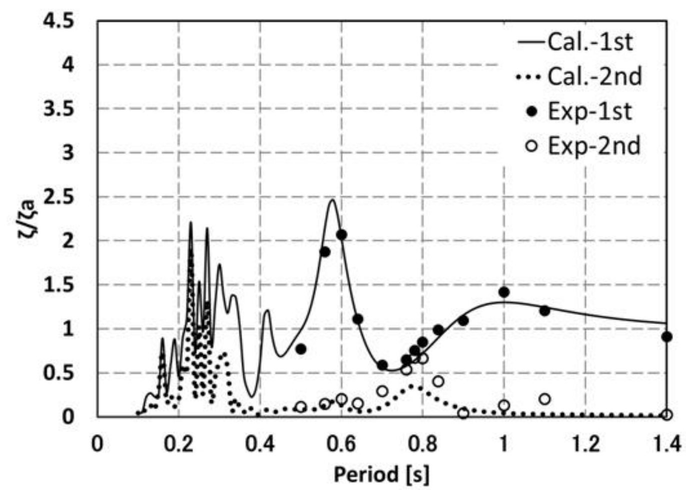

2 x 3 cylinders

WAMIT Computation

Draft=1 and water depth=4 are assumed

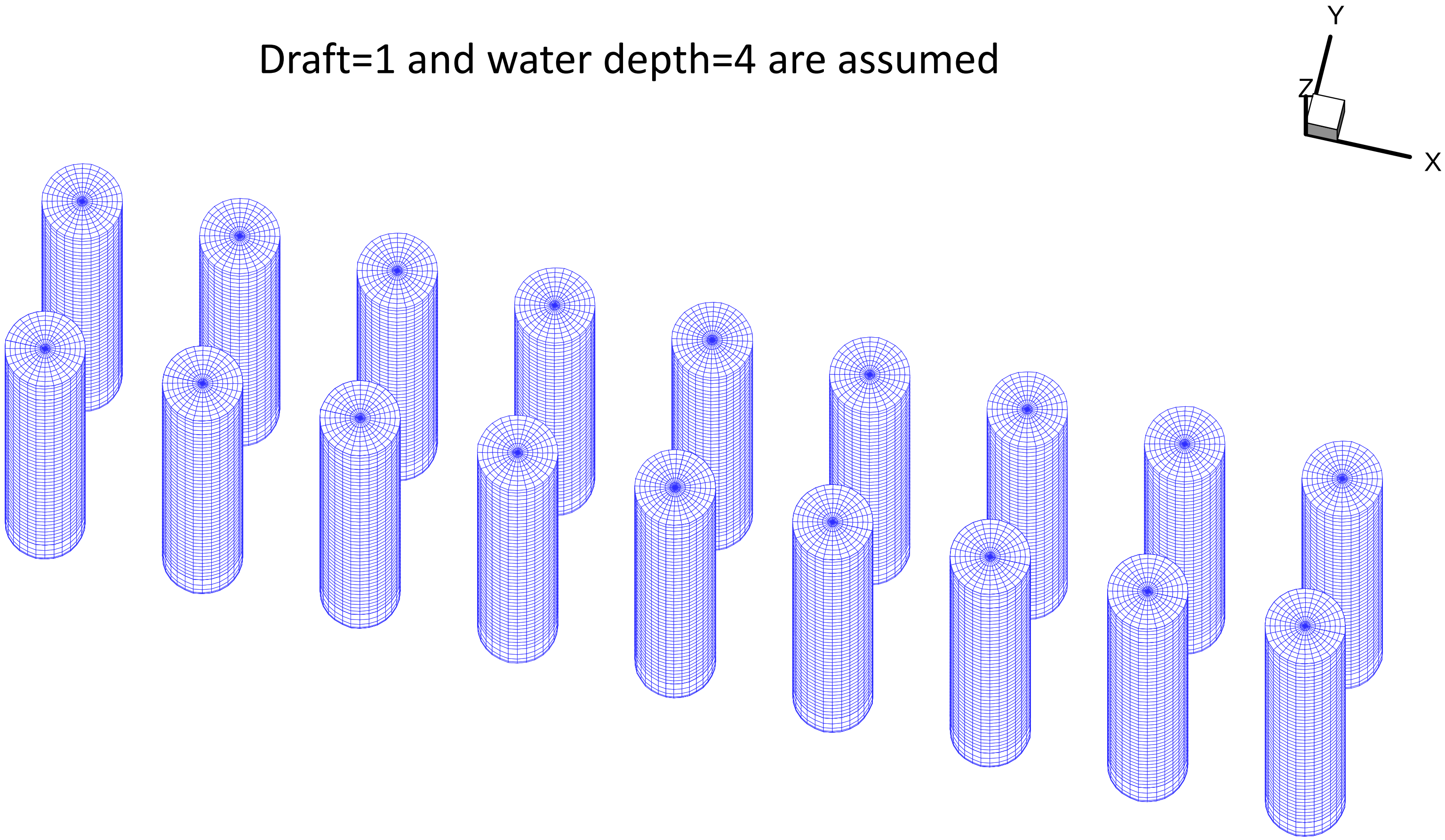

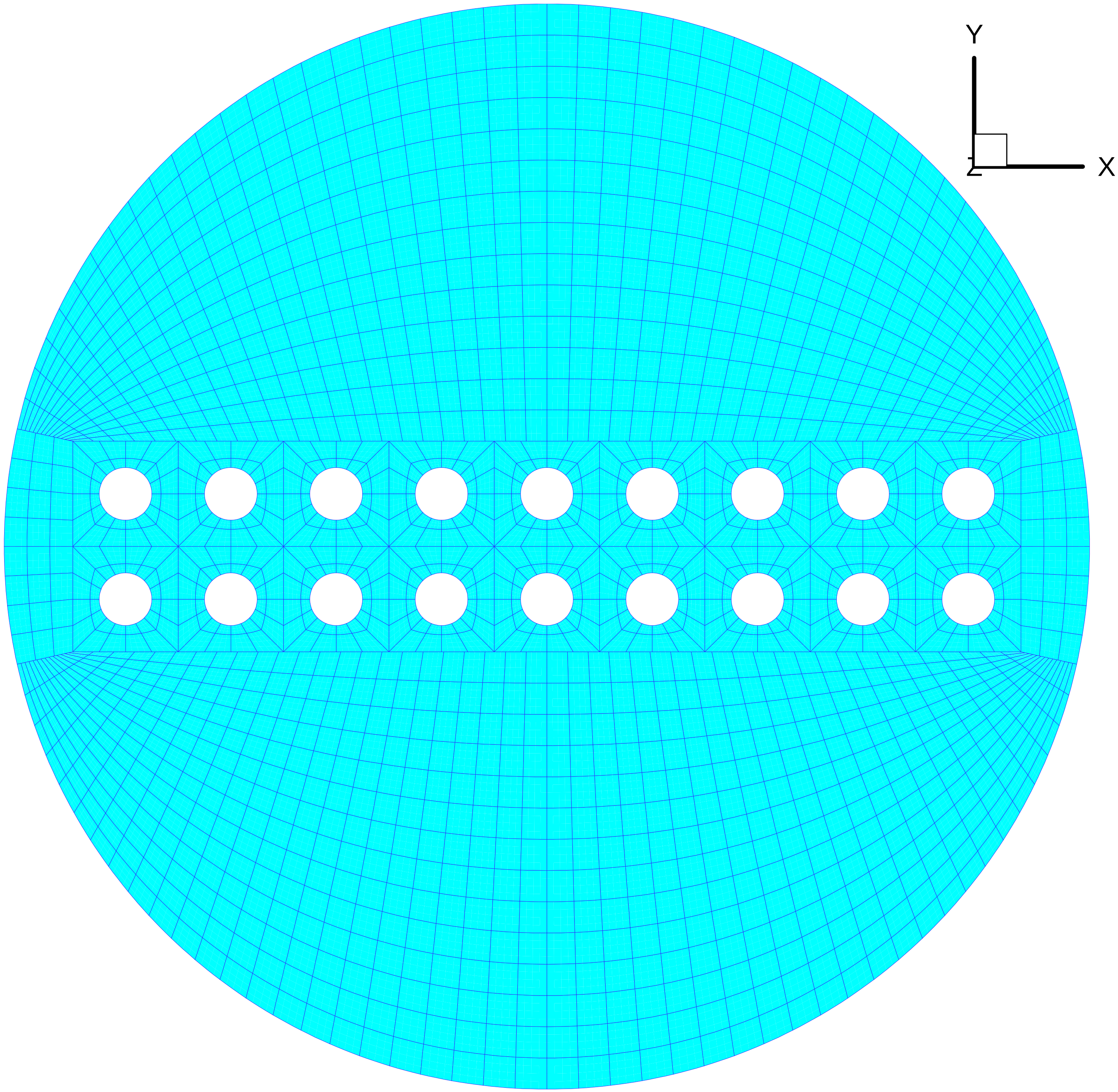
Y
X
Z

Kagemoto et al. (IWWWFB, 2014)

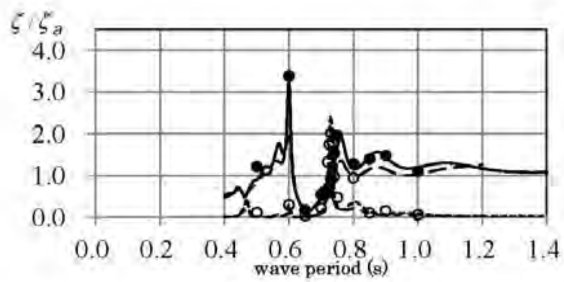

(a) Point A (H=20mm)

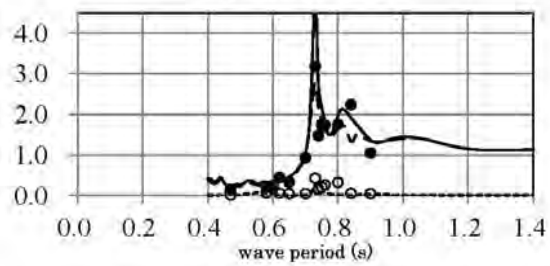

(b) Point B (H=10mm)

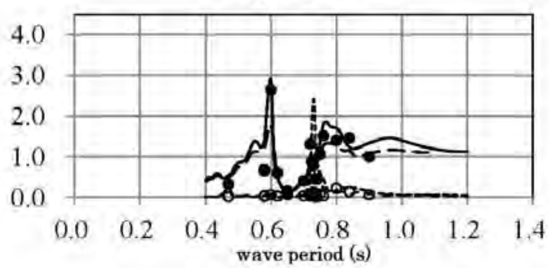

(c) Point C (H=10mm)

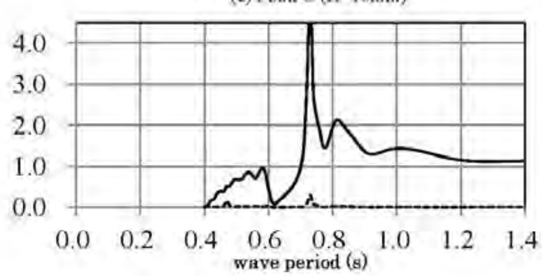

(d) Point D (H=10mm)

Fig.2 Experimental and theoretical results at Point A, B, C, & D (● Exp-1st, ○ Exp-2nd, —— Cal-1st, ... Cal-2nd, — — — Cal-1st (eps=0.03), - - - - Cal-2nd (eps=0.03))

WAMIT Computation (period increment 0.01sec)

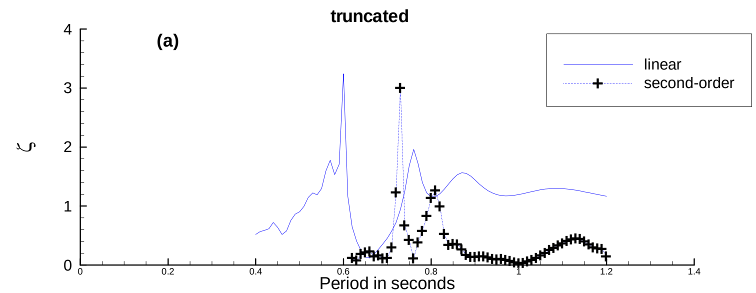

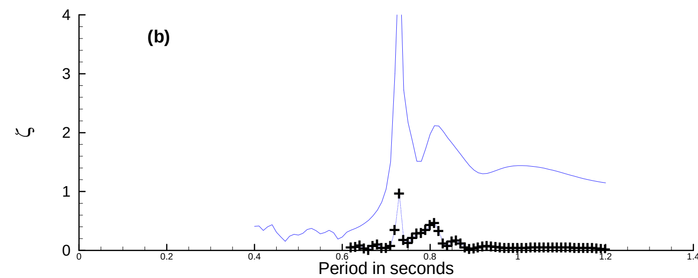

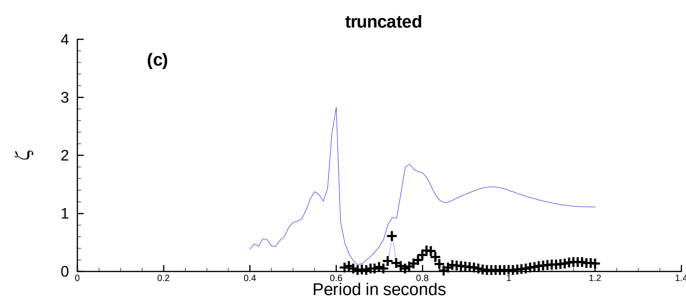

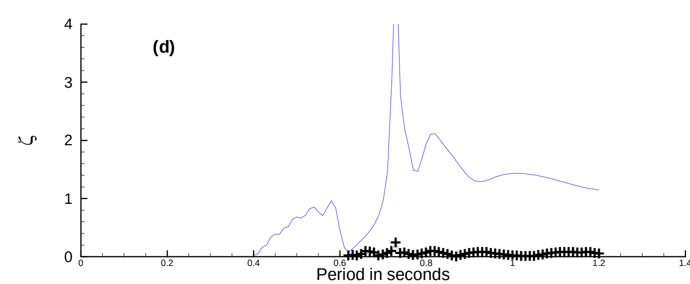

WAMIT Computation

(Period increment 0.02 sec)

Truncated. Draft=1 Depth=4

Bottom-mounted. Depth=1

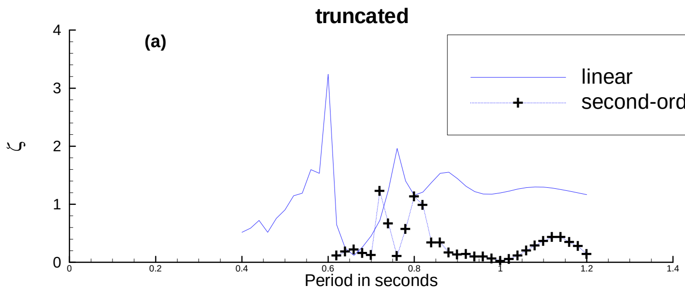

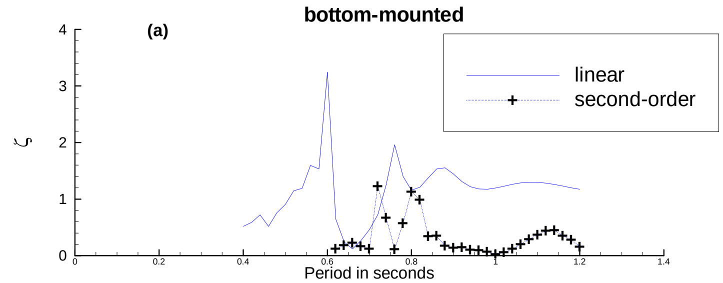

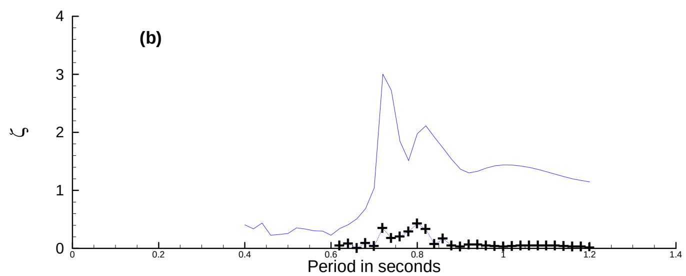

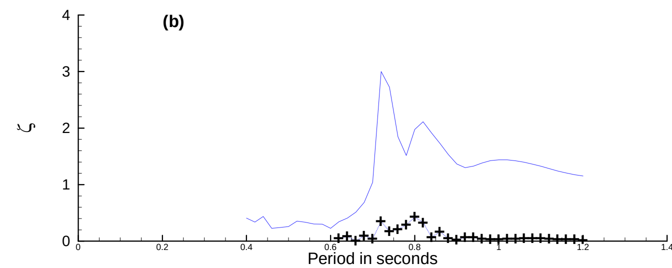

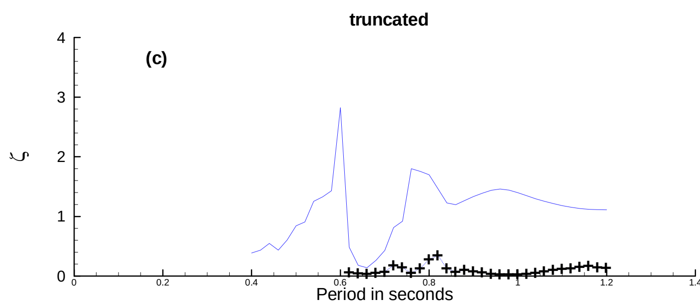

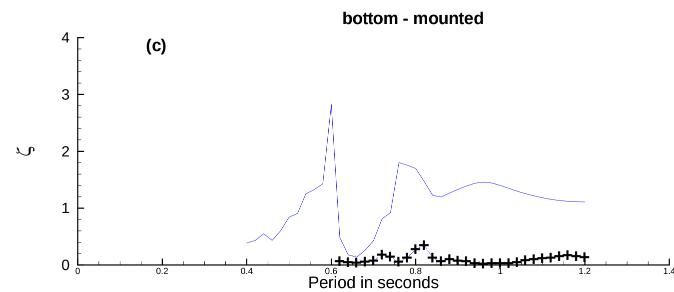

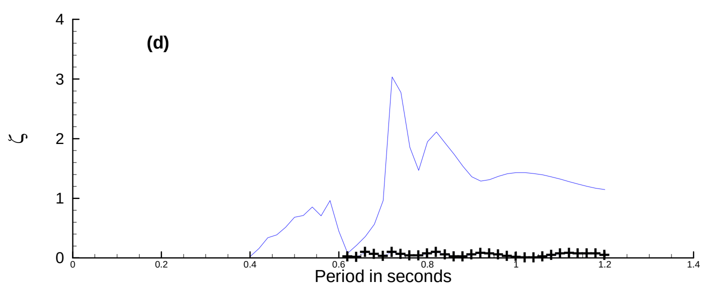

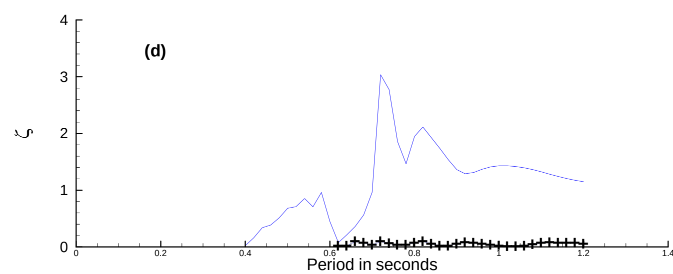

Summary on WAMIT computation of the wave elevation around an array of cylinders

- Computation predicts the peak periods accurately.

- Computed linear and second-order wave elevations are very close to the measurement except for the second-order wave elevation corresponding to the peak value at 0.73 seconds. This peak is narrowly banded.

- Between truncated and bottom mount cylinders, the computational results show no significant difference in both linear and second-order wave elevations.

- Further computation with exact water depth and the draft of the cylinder in the experiment is planned.

V70s Recent Progress

- Developed preliminary version

  Current V70s based on V7.06 and V6.49s

  ILOWHI=0 only

  - Take advantage of large RAM in data storage
  - Enable parallel processing with multiple processors
  - 1st-order codes replaced by V7 subroutines
  - 2nd-order code updated accordingly

2^{nd}-order Data storage in RAM

Major data storage for a routine 2^{nd}-order computation

- Real part of influence coefficients

  Q_{r2}=4*NLHS2*QLHS*(1+ILOG)*NEQN*NEQN

- Real part of influence coefficients on free surface

  Q_{f2}=4*6*NGEO*(1+ILOG)*NEQN*NTFS

- Complex components

  Q_{c2} =8*NLHS2*ISOR2*NEQN*NEQN

- Total RAM required

  Q_{r2}+Q_{f2}+NCPU*Q_{c2}

2nd-order Total Run time comparison

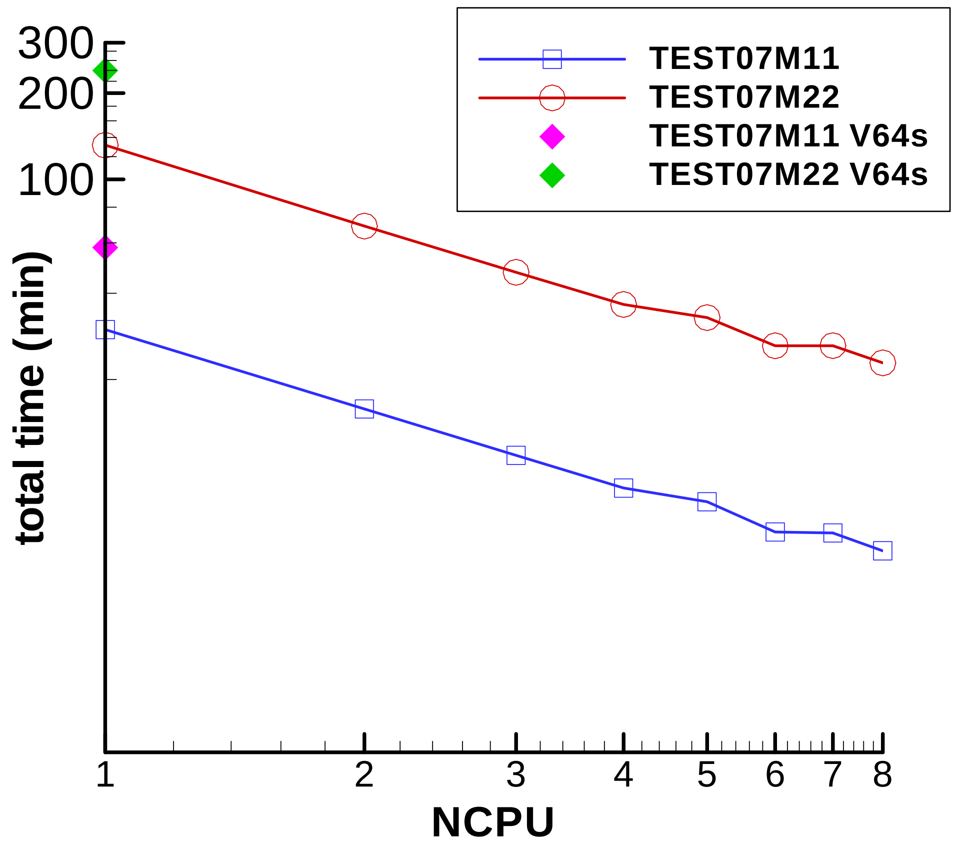

Modified TEST07.

TEST07M11: NEQN=2240, NTFS=1152

TEST07M22: NEQN=4224, NTFS=2376

NPER=36; NPER2=36, Direct and indirect method included

1st and 2nd-order run time comparison

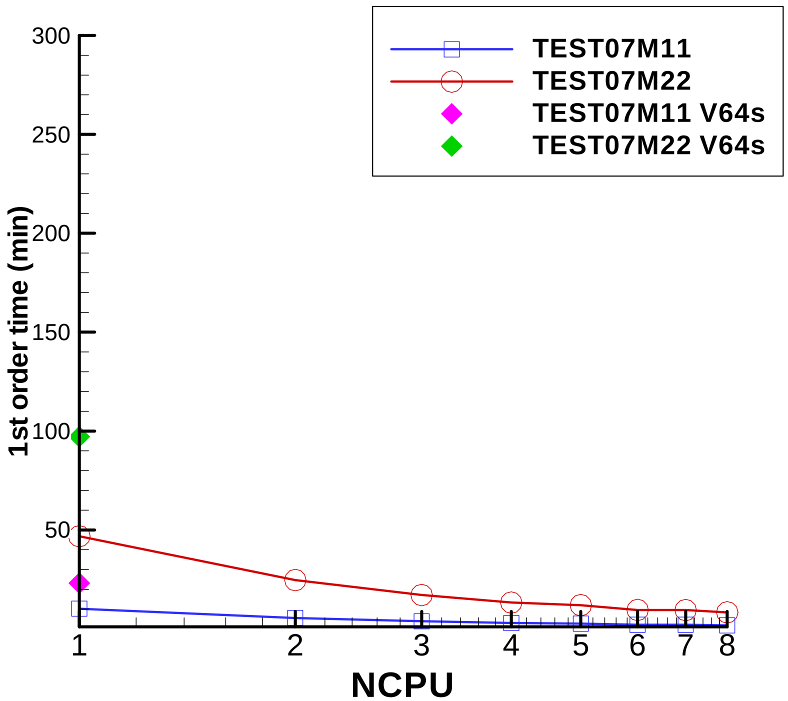

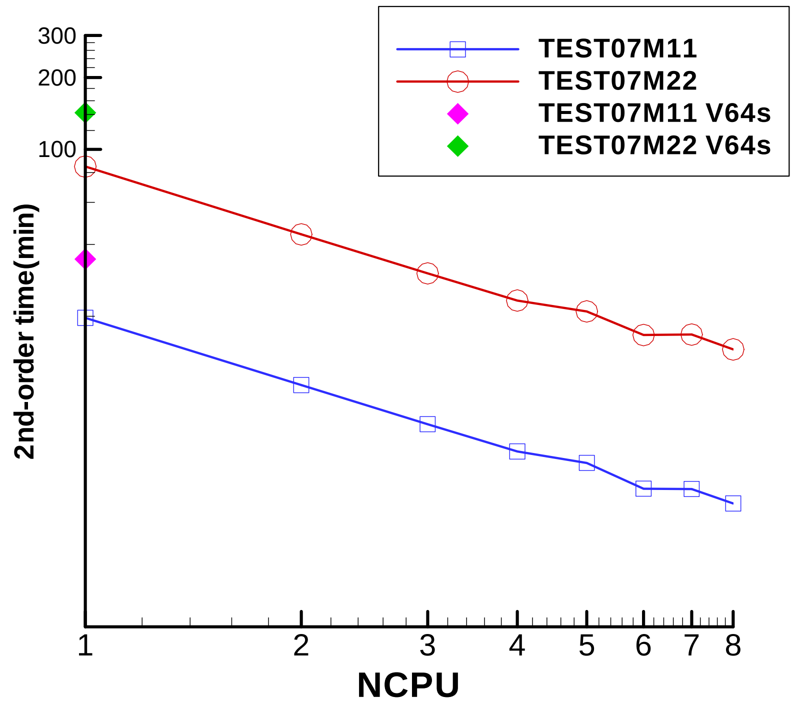

The test parameters are the same as in the previous page

Future Work

- Complete V70s coding using the newest V7 and V64s for low-order panel method (ILOWHI=0)
- Implement V70s for higher-order panel method (ILOWHI=1)
- Update V70s test cases & users manual

WAMIT v7.0 Information

- Linux Available
  - Site and lease licenses available
  - MultiSurf for WAMIT available (.rg2 files)
- HTML Manual on website
- Distributed via .msi file (Windows)

WAMIT Interface Development

- Input-based interface for the development of WAMIT input files
- Matlab driven interface

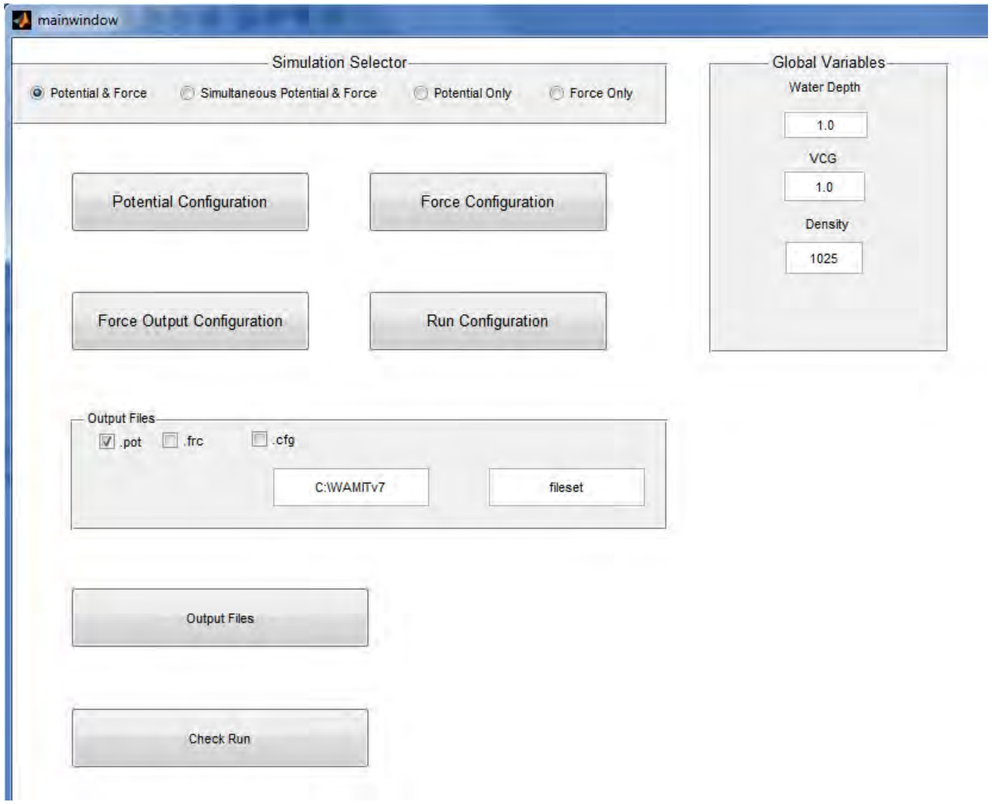

WAMIT Interface Development

- Provide a GUI-based platform for the development of input files
- Checks on inputs prior to WAMIT execution

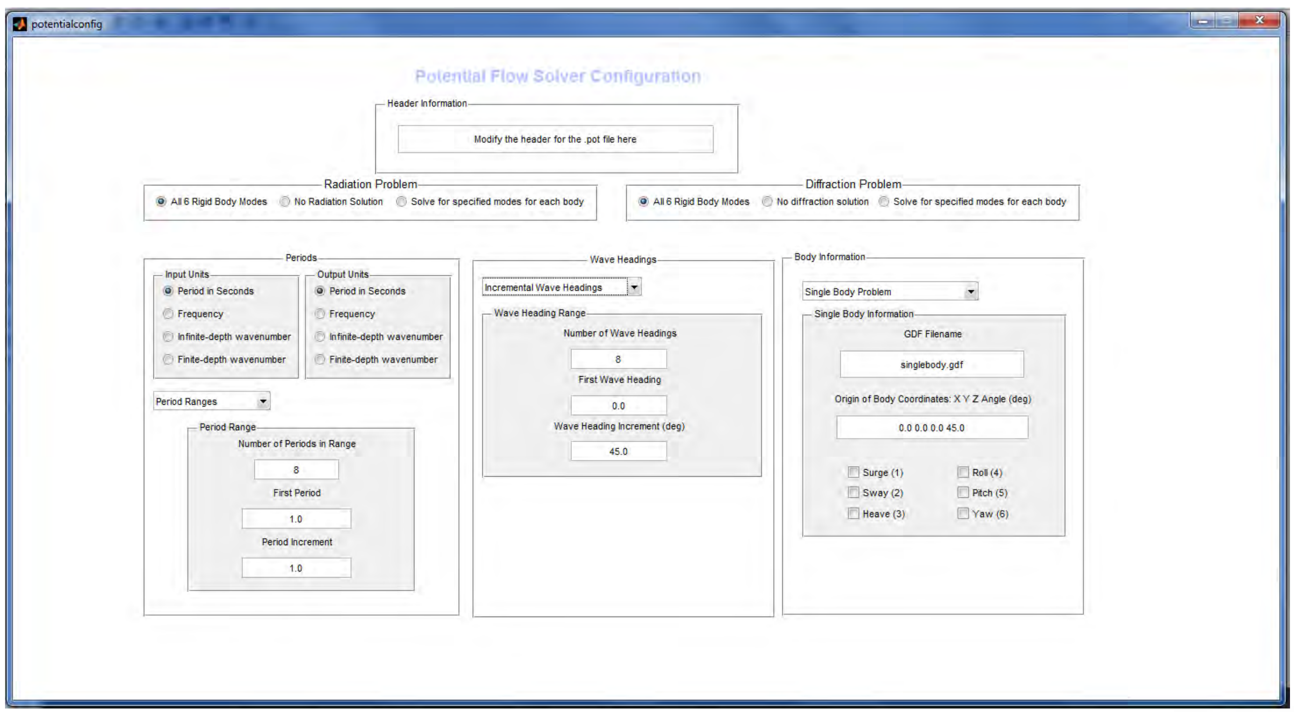

WAMIT Interface Development Status

- 75% complete
  - Single body problems
  - Generalized modes
  - Output options
- To do
  - Parameter verification
  - Multibody problems
  - Parsing existing input files

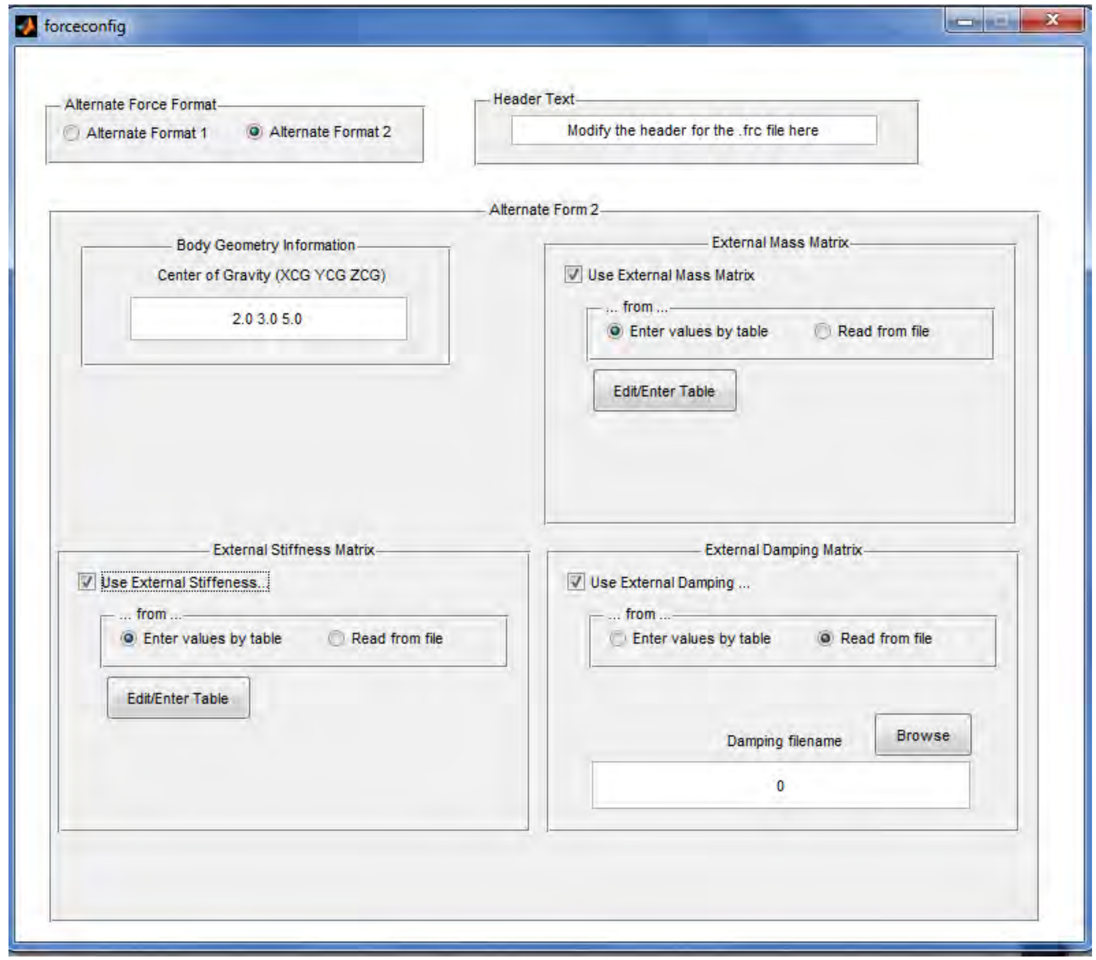

Plans for V71

(tentative release date 1 Jan 2015)

NEW PARAMTERS/OPTIONS in the cfg file (default values zero, except for NPFORCE):

- IDELFILES > 0: skip interactive I/O and delete old p2f and/or OUT fileS
  IDELFILES =1 delete old p2f file
  =2 delete old p2f and out files
  =3 delete old p2f and new p2f file
  =4 delete old p2f and new p2f file and old out file

- IOUTFNAME =1,2,3,4 add unique serial numbers to filename in .out and other output files,
  with 1,2,3 or 4 digits, e.g. if IOUTFNAME=2 and successive runs are made of test01 the out files will be named test01-nn where nn=01 to 99.
  This avoids the interactive I/O if an old out file exists and provides a sequential archive of all output files.
  (No old out files are deleted.)

- IOUTLOG=1 copy wamitlog.txt file to new file out_log.txt (prevents loss of wamitlog.txt and provides an achive of input files corresponding to the output files)

- IREADRAO=1,2 same as in V70
  IREADRAO=3 read data from columns 4,5 instead of 6,7 and convert modulus/phase to Re,Im
  in this case columns 6,7 are not required

- NPFORCE and NPNOFORCE are complementary (use one or the other but not both)
  NPNOFORCE defines panels or patches where the force integrations are skipped
  NPFORCE specifies panels or patches where the force integration is included, all others are skipped
  This feature can be used for structural loads such as shear, as a simpler alternative
  to using generalized modes

NEW OPTION IN POT FILE TO INPUT MULTIPLE GROUPS OF WAVE PERIODS:

- On the line normally used to input NPER the following optional line can be input:
  NPERGROUP = m
  NPERGROUP is not case sensitive and m is an integer. This line is followed by m groups of periods.
  Each group is input in one of the two formats explained in the user manual,
  either with nper>0 specified periods or with nper<0 to specify |nper| uniformly spaced periods.

OTHER EXTENSIONS/MODIFICATIONS:

- NEWMODES: Data files replace data in subroutines FREEBEAM_X and JACOBI to permit more general use (for bending modes of elastic structures)

WORK IN PROGRESS:

- More efficient evaluation of field outputs (options 6p, 6vx, ...) when NFIELD is VERY large. Motivated by applications where free surface animations are needed over large areas, particularly if NEQN is also large

Various bug fixes

Pressure surfaces.

A floating structure with an air cushion & oscillating water columns

Overview

- WAMIT V7 has an option to evaluate a radiation potential due to an oscillatory pressure over a horizontal area, S_f, a pressure surface, enclosed by an air chamber as in oscillating water columns (OWC) or air cushion vehicles(ACV)
- S_f may be on Z=0, the plane of the exterior free surface, or, Z <0 due to prescribed static pressure, as in ACV (or a submerged air chamber with free surface, S_f.)
- The oscillatory pressure in the chamber is driven by water waves and typically the air pressure is uniform in the chamber
- With uniform air pressure within a chamber, the number of additional modes is the same as the number of S_f (or number of air chambers). This is a simpler alternative to use of multiple generalized modes, such as Fourier modes to represent the free surface elevation on S_f.
- Varying pressure distribution due to acoustic waves in the chamber can be accounted for using more than one mode in each chamber but is not considered here.
- For ACV, motion of the vessel due to trapped air is of interest. The air is treated as a source of restoring force. For OWC, optimum extraction of power is of interest.

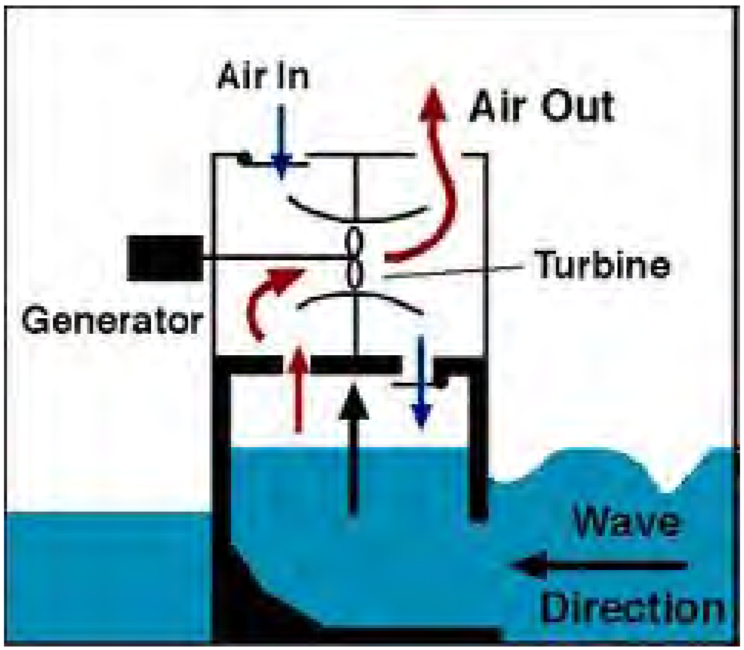
Air In
Air Out
Turbine
Generator
Wave
Direction

OWC

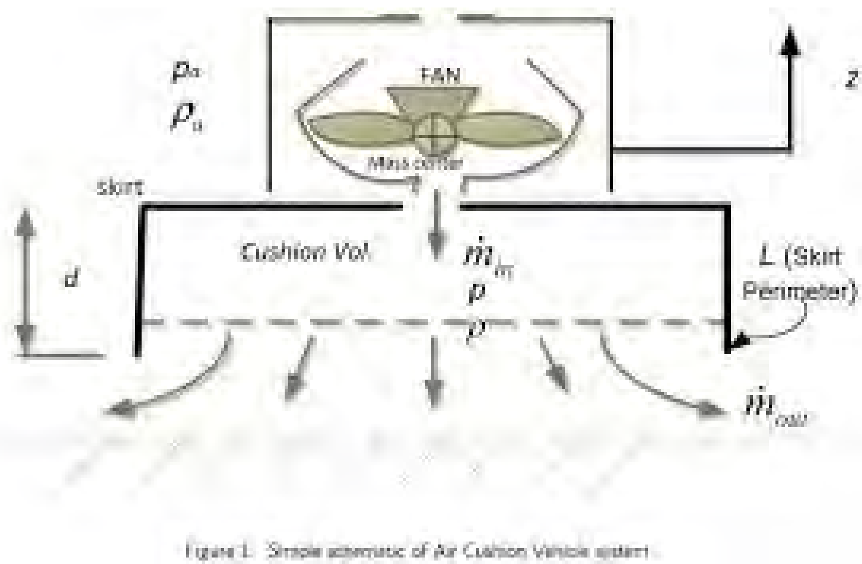
FAN
z
skirt
Cushion Vol.
d
L (Skirt
Perimeter)

ACV

Definitions and conventions

In the presense of M_p pressure chambers, the pressure distribution on S_f is represented by

$$p_0(x,y,z) = -\rho g \sum_{j}^{6+M_p} \xi_j n_j(x,y,z) \tag{1.1}$$

where $j=7$ corresponds to the first of S_f and $j=8$ the second and so on so forth. $n_7 = 1$ on the first of S_f and 0 on S_b, the body surface and on other pressure surfaces.

The complete velocity potential is given by the sum of the diffraction potential and radiation potentials. The latter consists of those corresponding to conventional 6 rigid body modes and one radiation potential for each pressure surface

$$\varphi = \varphi_R + \varphi_D, \tag{1.2}$$

$$\varphi_R = i\omega \sum_{j=1}^{6} \xi_j \varphi_j + \varphi_p = i\omega \sum_{j=1}^{6} \xi_j \varphi_j + i\omega \sum_{j=7}^{6+M_p} \xi_j \varphi_j \tag{1.3}$$

From the linearized Bernoulli equation, the pressures on S_f are

$$p_0(x, y, z) = -i\rho\omega\varphi(x, y, z) - \rho g\zeta(x, y, z) \tag{1.4}$$

where ρ is denisty of water, ω wave frequency, ζ wave elevation from the mean position.
As $\varphi_z = i\omega\zeta$, it follows that

$$\varphi_z - K\varphi = -\frac{i\omega}{\rho g}p_0 \quad \text{on} \quad S_f \tag{1.5}$$

where $K = \omega^2/g$.

φ_D and φ_j, for $j \leq 6$, are subject to the homogeneous free surface condition on S_f. φ_j, for $j \geq 7$, is then subject to

$$\varphi_{j_z} - K\varphi_j = n_j \quad \text{on} \quad S_f \tag{1.6}$$

and

$$\varphi_{j_n} = n_j = 0 \quad \text{on} \quad S_b \tag{1.7}$$

where S_b denotes the wetted body surface.

The radiation pressure forces, represented by the added-mass and damping coefficients are

$$A_{ij} - \frac{i}{\omega}B_{ij} = \rho \iint_{S_b+S_f} n_i\varphi_j dS \tag{1.8}$$

and the exciting forces are

$$X_i = -i\omega\rho \iint_{S_b+S_f} n_i\varphi_D dS \tag{1.9}$$

A structure with air cushions

A relation between the pressure and the volume in each chamber provides additional equations of motion. Total change of the air volume in k-th chamber is the sum of the change caused by the wave elevation

$$dv_1 = -\int_{S_f} \zeta n_i dS \tag{1.10}$$

and the vertical body motion

$$dv_2 = \int_{S_f} (\xi_3 + \xi_4 y - \xi_5 x) n_i dS = \xi_3 S_i + \xi_4 S y_i - \xi_5 S x_i \tag{1.11}$$

where $i = k + 6$, S_i, Sx_i and Sy_i are the area and the first moments in x and y of S_f, respectively, of the kth chamber.

For exampe, assuming adiabatic process, $pv^\gamma = PV^\gamma$ and small change of volume, we have a relation

$$p_o = -\gamma(P/V)dv = -C_p dv \tag{1.12}$$

where P is the static pressure including the atmospheric pressure and V is the mean air volume. For air, $\gamma = 1.4$.

From (1,1) and the definition of n_j, p_o in k-th chamber is

$$p_o = -\rho g \xi_i \tag{1.13}$$

Combining (1.10), (1.11), (1.12) and (1.13), we can write the equation of motion derived from the k-th chamber

$$0 = \frac{\rho g}{C_p}\xi_i - S_i \xi_3 - S y_i \xi_4 + S x_i \xi_5 + \int_{S_f} \zeta n_i dS \tag{1.14}$$

Inserting the wave elevation in (1.4) to (1.14), along with the pressure in (1.13) and the velocity potentials in (1.2) and (1.3), we have

$$\sum_{j=1}^{6+M_p} [-\omega^2 A_{ij} + i\omega B_{ij} + C_{ij}]\xi_j = X_i \tag{1.15}$$

The hydrostatic coefficient $C_{ij} = 0$ except when $j = 3, 4, 5$ and i and it can be shown C_{ij} are symmetric. Nonzero hydrostatic coefficients are

$$C_{i,3} = C_{3,i} = \rho g S_i \tag{1.16}$$

$$C_{i,4} = C_{4,i} = \rho g S y_i \tag{1.17}$$

$$C_{i,5} = C_{5,i} = -\rho g S x_i \tag{1.18}$$

$$C_{i,i} = -\rho g S_i - \frac{(\rho g)^2}{C_p} \tag{1.19}$$

In a simpler model, where $dv = dv_1 + dv_2 = 0$ without considering the compressibility of air, the first term of the right-hand side of (1.14) and the second term on the righ-hand side of (1.19) vanish.

An example: a model used by Pinkster (BOSS, Delft, 1997) in an experiment and computational analysis. Computation was also made by Lee and Newman (VLFS Conf., 1999).

Length 2.5m, beam=0.78m and draft 0.15m

Wall thickness 0.02m at the ends and 0.06m at the sides

The air chamber extends from 0.05m below the exterior free surface to 0.13m above with the volume V=0.292248 m^3

Center of gravity is at (0,0,0.15). Pitch radius of gyration is 0.751. Radius of gyration about (0,0,0) is 0.76583353.

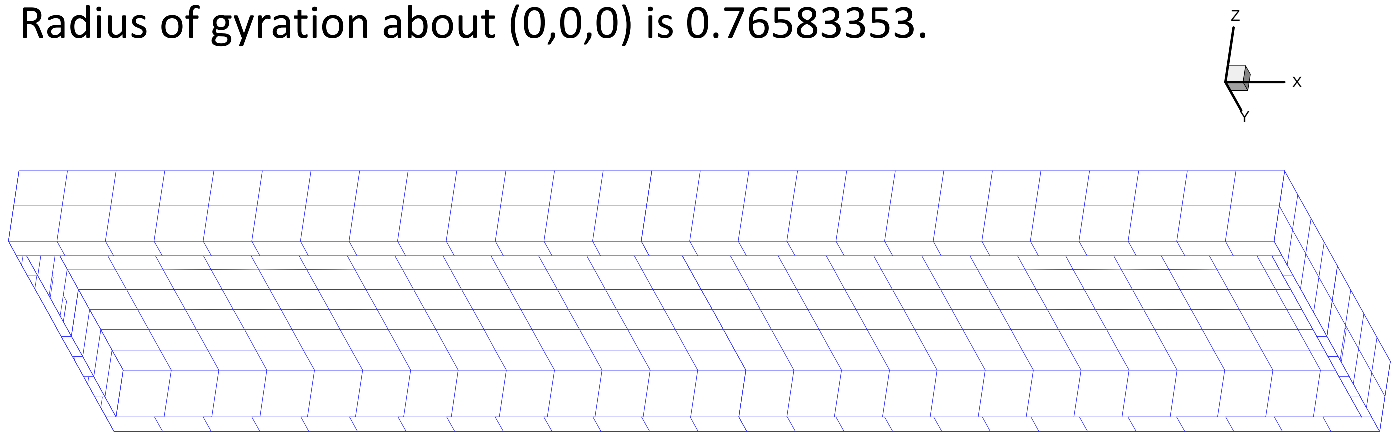

After normalized by water density.

- Mass = 0.13014
- Pitch moment of inertia = 0.07632722
- S_i =1.6236
- C(3,7)=C(7,3)=15.92208
- C(7,7) =-15.92208

Compressibility is not considered.

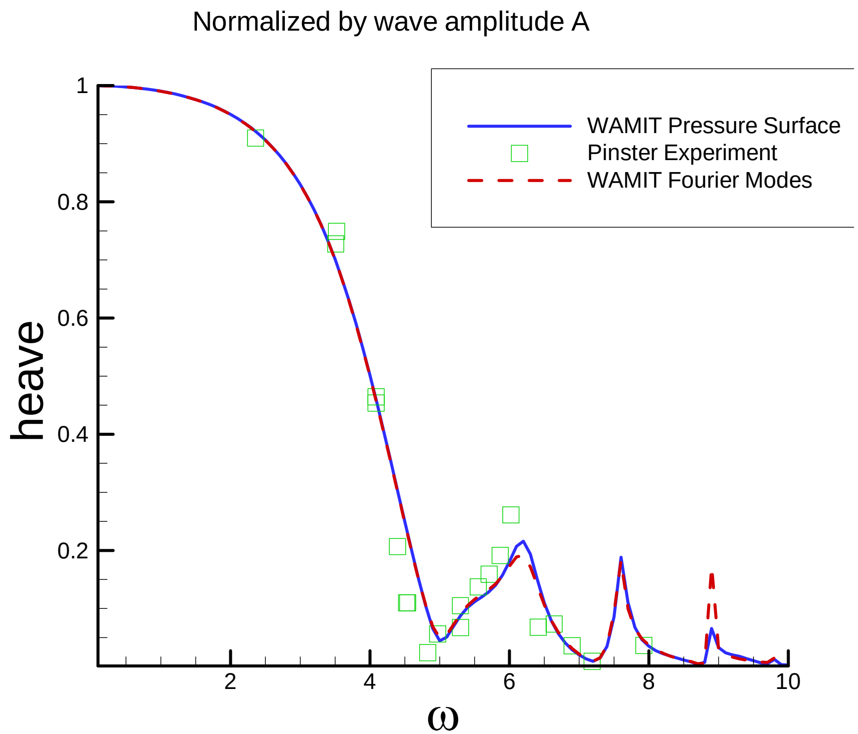

Normalized by wave amplitude A
heave
ω
WAMIT Pressure Surface
Pinster Experiment
WAMIT Fourier Modes
1
0.8
0.6
0.4
0.2
2
4
6
8
10

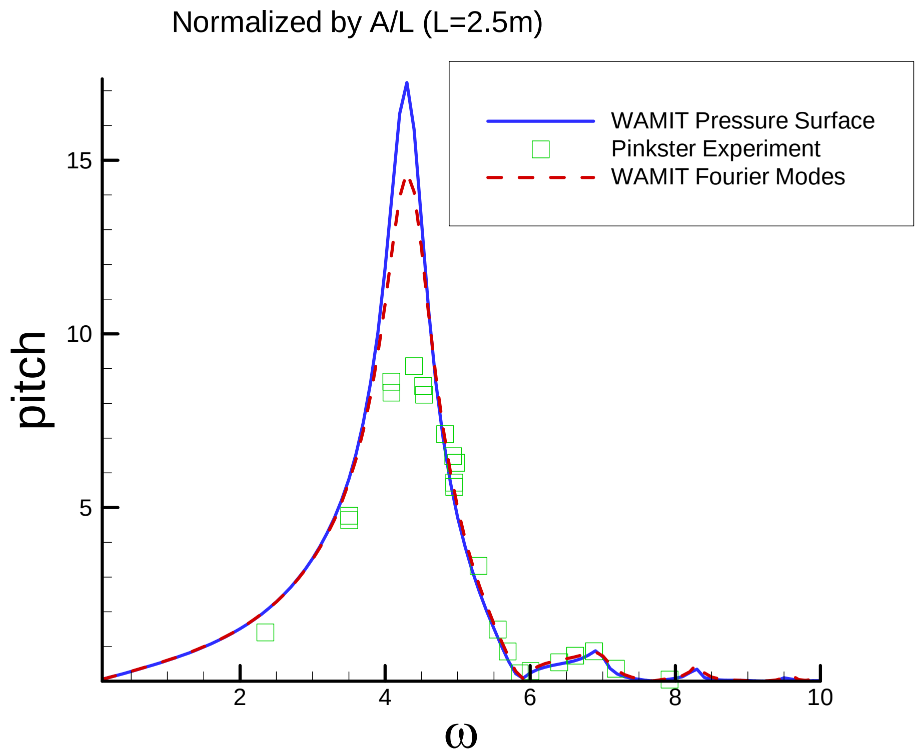

Normalized by A/L (L=2.5m)
pitch
ω
WAMIT Pressure Surface
Pinkster Experiment
WAMIT Fourier Modes
15
10
5
2
4
6
8
10

When the effect of the air turbine is considered by a linear relationship of the air flux and the pressure

$$\int_{S_f} \varphi_z dS = B_{0j} p_0 \tag{1.20}$$

we have an equation of motion in the form

$$\sum_{j=1}^{6+M_p} [-\omega^2 A_{ij} + i\omega(B_{ij} + B_{i,j}^E) + C_{ij}]\xi_j = X_i \tag{1.21}$$

by inserting the velocity potentials in (1.2) and (1.3) and the pressure in (1.13) to (1.20). In (1.21), $B_{ij}^E = 0$ and $C_{ij} = 0$ except

$$B_{ii}^E = \frac{(\rho g)^2 B_{0i}}{\omega^2} \tag{1.22}$$

$$C_{ii} = -\rho g S_i \tag{1.23}$$

Summary

- Two applications are discussed to illustrate the use of the pressure mode. The equations of motion for the pressure modes are derived to have appropriate constraints (external force matrices) for particular applications.

- For similar applications, a set of modes, such as Fourier modes ,had to be used to represent the free surface. This procedure is significantly simplified by replacing a set of modes with one pressure mode for each uniform pressure surface.

- Note: The computation is made using a WAMIT version under – development.

Current Participants

ConocoPhillips

OTRC

Petrobras/USP

Shell

Statoil

Scott Coblitz
ConocoPhillips Company
600 N Dairy Ashford Rd, Office MO-01-1022
Houston, TX 77079
scott.e.coblitz@conocophillips.com

Tyler Groll
University of Michigan
tgroll@umich.edu

Kelli Hendrickson
WAMIT
822 Boylston Street, Suite 202
Chestnut Hill, MA 02467
kelli@wamit.com

Chang-Ho Lee
WAMIT
822 Boylston Street, Suite 202
Chestnut Hill, MA 02467
chlee@wamit.com

Nathaniel Meredith
University of Michigan
nmeredit@umich.edu

Nick Newman
WAMIT
1 Bowditch Road
Woods Hole, MA 02543
jnn@mit.edu

John Niedzwecki
709A CE/TTI
Zachry Department of Civil Engineering
Texas A&M University
3136 TAMU
College Station, TX 77843-3136
j-niedzwecki@tamu.edu

Robert Page
AeroHydro
54 Herrick Road/PO Box 684
Southwest Harbor, ME 04679-0684
robertpage@aerohydro.com

Xuemei Zhu
WAMIT
822 Boylston Street, Suite 202
Chestnut Hill, MA 02467
xmzhu@wamit.com

Past Participants

Rolf Baarholm
Statoil ASA
Arkitekt Ebbels veg 10
Rotvoll, Trondheim
Norway
rolbaa@statoil.com

Job Baar
Shell International Exploration and Production Inc.
Room 5146, Woodcreek
200 North Dairy Ashford Rd, Houston, TX 77079, USA
Tel: +1 281-5444344
Job.Baar@shell.com

Donald Danmeier
Chevron Energy Technology Co.
6001 Bollinger Canyon Road
Room L-4220
San Ramon, CA 94583-2324
DDanmeier@chevron.com

Marcos Ferreira
Petrobras SA
Eng. Marcos Donato Ferreira
CENPES/PDP/MC
Av Horacio Macedo, 950
Cidade Universitaria, Ilha do Fundao
21941-915
Rio de Janeiro, Brazil
marcos.donato@petrobras.com.br

Stergios Liapis
Shell Oil Company
Offshore Structures
3737 Bellaire Blvd.
Houston, TX 77025
stergios.liapis@Shell.Com

Yile Li
Shell International Exploration and Production Inc.
Room 5130, Woodcreek
200 North Dairy Ashford Rd, Houston, TX 77079, USA
Tel: +1 281-5444666
Yile.Li@shell.com

Edgard Malta
Department of Naval Architecture & Ocean Engineering
Numerical Offshore Tank - TPN
Av. Prof. Mello Moraes, 2231, Cidade Universitária
CEP05508-900, SP, SP, Brazil
Edgard@tpn.usp.br

Rick Mercier
Offshore Technology Research Center
1200 Mariner Drive
College Station, TX 77845-3400
rmercier@civil.tamu.edu

Amal C. Phadke
ConocoPhillips Company
600 N Dairy Ashford Rd, Office MO-01-1022
Houston, TX 77079
amal.c.phadke@conocophillips.com

Joao Sparano
University of Sao Paulo
Numerical Offshore Tank
Department of Naval Architecture and Ocean Engineering
Av. Prof. Mello Moraes, 2231
Cidade Universitaria
Sao Paulo, SP, Brazil CEPO05508-900
5511 3091-1704 ext. 250
sparano@usp.br

Per Teigen

Statoil	Street Address
Postuttak	Ark, Ebbels v.10
N 7005 Trondheim	Rotvoll
Norway	Trondheim, Norway

pte@statoil.com

John Letcher
AeroHydro
54 Herrick Road/PO Box 684

Southwest Harbor, ME 04679-0684
jletcher@aerohydro.com

Rune Yttervik
Statoil ASA
Research Centre, Bergen
Norway
Rune.Yttervik@statoil.com

Tim Finnigan
Chevron Energy Technology Co.
6001 Bollinger Canyon Road
Room L-4296
San Ramon, CA 94583-2324
TimFinnigan@Chevron.com

Finn Gunnar Nielsen
Statoil ASA
PO Box 7190
N-5020 Bergen, Norway
Street Address
Sandsliveien 90
N-5254 Sandsli, Norway
Finn.Gunnar.Nielsen@statoil.com

Kazuo Nishimoto
Kazuo Nishimoto, Prof. Dr.
Department of Naval Architecture & Ocean Engineering
EPUSP
Numerical Offshore Tank - TPN
Av. Prof. Mello Moraes, 2231, Cidade Universitária
CEP05508-900, SP, SP, Brazil
knishimo@usp.br

Michael Shook
AeroHydro
54 Herrick Road/PO Box 684
Southwest Harbor, ME 04679-0684
mshook@aerohydro.com

George Gu
ConocoPhillips
MO-01-1020
600 North Dairy Ashford
Houston, TX 77079
george.z.gu@conocophillips.com